

# Induction of alpha-Amylase in Wheat Grain Cultivars as an Indicator of Resistance to Pre-harvest Sprouting

Aidar A. Khakimzhanov, Vladimir A. Kuzovlev, Nurgul S. Mamytova, Dinara A. Shansharova, Oleg V. Fursov

**Abstract**—The influence of humidity and low temperature on the  $\alpha$ -amylase activity and isoenzyme composition of grains of different wheat varieties have been studied. The identified samples of varieties have significant difference in the level of enzyme induction under the impact of high humidity and low temperature. It is proposed to use this methodological approach for testing genotypes and wheat breeding lines for resistance to pre-harvest sprouting (PHS).

**Keywords**— $\alpha$ -Amylase, isoenzymes, wheat, pre-harvest sprouting

## I. INTRODUCTION

**I**N a number of climatic zones of Kazakhstan in the adverse weather conditions such as high air and soil humidity (in the rainy seasons) the PHS has been observed in the wheat grain during the ripening and harvesting periods, which results in a significant deterioration in baking properties of wheat, and even utter uselessness of wheat for bakery in some cases [1]. One of the most distinctive features of sprouted grain is the increased  $\alpha$ -amylase activity [2]. Germination of grain during maturity or storage period is induced by a synthesis of specific forms of the enzyme, termed the "malt" or "germination"  $\alpha$ -amylase, which leads to hydrolysis of starch granules, the formation of water soluble dextrins, and, ultimately, the crude baked bread [3], [4]. It is established that exposure of wheat to PHS depends on the wheat genotype [5]. This fact opens the prospects for breeding for resistance to this factor. Together with the breeders from Kazakh Research Institute of Agriculture, based on electrophoretic detection of "germination"  $\alpha$ -amylase of more than 200 samples of wheat we have obtained a PHS-resistant cultivar, Lutescens 70.

Although, as a number of studies in recent years show, a resistance or a susceptibility to germinate in wheat grain is a multifactorial trait, which is associated not only with non-controlled synthesis of "germination"  $\alpha$ -amylase in the maturing grain. A number of Australian scientists' studies [6], [7] demonstrated the existence of an enzyme with high isoelectric points (pI) in a number of late maturity  $\alpha$ -amylase (LMA) genotypes.

These authors found that the LMA form of the enzyme in wheat is a result of a genetic defect that leads to the accumulation of high activity  $\alpha$ -amylase with high pI in the ripening seeds in the absence of conditions for germination (high humidity) or other environmental factors. In the UK the LMA enzyme is also termed as pre-maturity  $\alpha$ -amylase (PMAA) [8]. These authors emphasize that the LMA or PMAA enzyme is a result of a genetic defect that is present in some wheat genotypes, which can be spread around the world through negligent breeding programs. This  $\alpha$ -amylase, synthesized in the maturing grain, maintains or increases its activity due to storage temperature (about +12<sup>0</sup> C), which subsequently leads to low falling number (FN) index and adversely affects on the quality of the end-product i.e. bread [9], [10].

In addition to the revealed factors of the resistance/susceptibility to PHS we have identified another factor – a low content of phytohormone abscisic acid (ABA) in grain [11]. As it is known, the ABA being antagonist to gibberelic acid, inhibits the synthesis of "germination"  $\alpha$ -amylase and contributes to the preservation of seed in the dormant state [12]. Our studies have shown that PHS-resistant Lutescens 70 cultivar contains more ABA than susceptible Novosibirskaya 67.

Thus, this brief review points to a genetic dependence and multifactorial resistance to PHS. The significance of the research topic is confirmed by the development of international and national genetic programs aimed at understanding this phenomenon and the search for resistant genotypes [13], [14].

In this work we have investigated the influence of artificial model conditions that encourage the sprouting process in close to the climatic conditions of main grain producing regions of Kazakhstan on the activity and isoenzyme spectra of  $\alpha$ -amylase of various soft wheat grains in order to identify varieties and breeding lines that are resistant to pre-harvest sprouting.

## II. MATERIALS AND METHODS

### A. Seed Material

The study examined several varieties of soft spring wheat: (*Triticum aestivum* L.), cultivated in Kazakhstan (Saratovskaya 29, Kazakhstanskaya 10, Kazakhstanskaya rannya, Kaiyr, Almaken, Yrym, Lutescens 70, Lutescens 157, Lutescens 314, Lutescens 462), and the promising breeding

A.A. Khakimzhanov, V.A. Kuzovlev, N.S. Mamytova and O.V. Fursov are with the Institute of Molecular Biology and Biochemistry, Almaty, Kazakhstan (e-mail: aidar1611@gmail.com).

D.A. Shansharova is with the Faculty of Food Technology Almaty Technological University, Kazakhstan.

lines (no.132 winter, no.132 spring, no.138 winter, no.132 spring) harvested in 2007 from the fund of Kazakh Research Institute of Agriculture.

#### B. Experimental Conditions

To modeling the provocative conditions of sprouting, freshly harvested wheat heads of fully ripe stage of the studied cultivars and breeding lines were placed in a climate chamber KBWF240 (Binder, Germany) with controlled temperature and humidity. Day and night time temperatures were 18<sup>o</sup> and 10<sup>o</sup>C respectively at a constant humidity of 80%. The wheat heads served as controls, which were stored at room temperature. The procedures of treatment (humidification and cooling) imitated the weather conditions with low temperature and high humidity during the harvest season, typical for the northern regions of Kazakhstan.

#### C. Alpha-Amylase Studies

At the day 3, 7 and 11 the total amylase and  $\alpha$ -amylase activity in the control and experimental (subjected to treatment) grains have been determined by starch-iodine method [15]. Isoelectric focusing (IEF) of  $\alpha$ -amylase was carried out on 1 mm plates 5% polyacrylamide gel (PAG) in a gradient of Pharmalyte pH 4-9 (Pharmacia, Sweden). Upon the completion of IEF PAG-plates were incubated in 1.5% starch solution for 1 hour at +4<sup>o</sup>C, followed by staining of zones activity of the enzyme by J<sub>2</sub>/KJ solution.

### III. RESULTS AND DISCUSSIONS

The variability of the grain amylase activity after the treatment by low temperature and high humidity at the day 3, 7 and 11 has been investigated in the study. The data presented in TABLE 1 indicates the stimulating effect of grain treatment on the overall ( $\alpha + \beta$ ) amylase activity. Moreover, a significant (more than 10-fold) increase in amylase activity in grain was observed only in some varieties (Saratovskaya 29, Kazakhstanskaya 10, Lutescens 462 and no.138 winter). Other variety samples (Yrym, Lutescens 70 and Lutescens 314) differed by significantly lesser increase (2.0 - 3.5 times) in total amylase activity by the day 11 of the treatment.

As noted, the effect of sprouting, caused by the conditions of ripening or storage of wheat grain is associated with the synthesis of  $\alpha$ -amylase. In this regard, a study also examines the variability of this enzyme activity by the action of low temperature and high humidity (TABLE 2).

The data presented in TABLE 2 also shows the growth of  $\alpha$ -amylase activity caused by the treatment. In control samples the activity of  $\alpha$ -amylase was minimal and did not change significantly from the storage period.

The greatest increase in activity of  $\alpha$ -amylase compared to control at the 11th day of treatment was showed by the following cultivars and breeding lines: Saratovskaya 29 (412 fold), Kazakhstanskaya 10 (148 fold), Lutescens 462 (173 fold), no.132 winter (116 fold), no.132 spring (105 fold) and Kaiyr (140 fold). More stable and resistant to treatment were the following cultivars: Yrym (40 fold), Lutescens 70 (93 fold), Lutescens 314 (21 fold), Lutescens 157 (74 fold) and no.

138 winter (32 fold). From the TABLE 2 it can be inferred that there are differences in the resistance of wheat genotypes to sprout, i.e., the presence of some endogenous factors that prevent the uncontrolled synthesis of  $\alpha$ -amylase in provocative conditions. In order to determine the contribution of different groups of  $\alpha$ -amylase isoenzymes in forming the overall amylase and  $\alpha$ -amylase activity under provocative conditions we studied the enzyme IEF spectra by the stages of treatment (Fig.1, a). In the spectra of control samples only the activity of low pI isoenzymes (Group A), the so-called "green" forms of  $\alpha$ -amylase [16] has been revealed. The presence of this group in a resting grain of control samples is due to the fact that the grain was taken for analysis in the late stages of ripeness, so these isoforms probably did not went into a latent state. Increased activity of  $\alpha$ -amylase after exposure to provocative conditions associated with the induction of "germination"  $\alpha$ -amylase isozymes of groups B and C (Fig.1, b, c, d). Moreover, it is clear that the samples differed in the dynamics of these  $\alpha$ -amylase isoenzymes synthesis.

The greatest differences between the studied cultivars and breeding lines in the isozyme spectra of  $\alpha$ -amylase induced by treatment, were observed on the day 7 (Fig.1, c). The maximum activity of "germination"  $\alpha$ -amylase isoenzymes were exhibited by Saratovskaya 29, Kazakhstanskaya 10, Lutescens 462, which differed from other varieties by the high enzyme activity (TABLE II). Less heterogeneous were isozyme spectra of Yrym, Lutescens 70, Lutescens 314, Lutescens 157 and no. 138 winter. By the end of the treatment period (the day 11) the differences between the samples for isozyme composition of "germination"  $\alpha$ -amylase have been leveled due to high specific activity of the enzyme at this stage of treatment. Despite this, the differences in the isozyme compositions of  $\alpha$ -amylase with high pI (Group C), which exhibited its activity at the day 7 of treatment, were still visible (Fig.1, c, d). It is not excluded that it may be associated with the presence of above mentioned LMA form of the enzyme in certain genotypes. More detailed studies on the possibility of the presence of LMA form of  $\alpha$ -amylase in genotypes of wheat grown in Kazakhstan are the subject of our further work.

### IV. CONCLUSION

Thus, among the studied wheat cultivars we have identified resistant and non-resistant to the external factors of  $\alpha$ -amylase induction, i.e. to the PHS or sprouting during the storage. Non-resistant to these effects varieties and breeding lines differed by accelerated dynamics of the synthesis of "germination"  $\alpha$ -amylase isoenzymes. More resistant to the induction of the enzyme cultivars can provide a good basis for breeding for resistance to sprouting.

### REFERENCES

- [1] Khaydarova J.S., Morunova T.M., Fursov O.V., Darkanbaev T.B. Amylase activity and some technological properties of wheat. J. Appl. biochemistry and microbiology. 1983. V.19. № 4. P. 435-446.
- [2] Kozmina N.P. Biochemistry of grain and its end-products. Moscow: Nauka, 1976. 374p.

- [3] Kruger J.E. Biochemistry of pre-harvest sprouting in cereals and practical application in plant breeding. *Cereal Res. Commun.*, 1976. V.4. P.187-194
- [4] Mansour K. Sprout damage in wheat and its effect on wheat flour product. In: Walker-Simmons M.K., Ried J.L. (eds) *Preharvest sprouting in cereals*. 1992. P. 8-9
- [5] Flintham J.E., Gale M.D. Genetic of preharvest sprouting and associated traits in wheat: review. *Plant Varieties and Seeds*. 1987. V.1. P. 87-97.
- [6] Mares D.J., Gale M.D. Control of  $\alpha$ -amylase synthesis in wheat grains. In: Ringland K., Mosleth E., Mares D.J. eds. *Proceeding of the fifth international symposium on preharvest sprouting in cereals*. Boulder, Colorado: Westview Press. 1990. P.183-194
- [7] Mrva K., Mares D.J. Control of late maturity  $\alpha$ -amylase synthesis compared to enzyme synthesis during germination. In: Noda K., Mares D.J. eds. *Proceeding of the seventh international symposium on preharvest sprouting in cereals*. Osaka. Japan: Center for Academic Societies. 1996. P. 419-426
- [8] Gale M.D., Flintham J.E., Arthur E.D. Alpha-amylase production in the late stage of grain development: an early sprouting damage risk? In: Kruger E.J., LaBerge E.D. eds. *Third international symposium on preharvest sprouting in cereals*. Boulder. Colorado: Westview Press. 1983. P.29-35
- [9] Mrva K., Mares D.J. Induction of late maturity  $\alpha$ -amylase in wheat by cool temperature. *Australian J. Agr. Res.* 2001. V.52. P.477-484
- [10] Mares D., Mrva K. Late-maturity  $\alpha$ -amylase: low falling number in wheat in the absence of preharvest sprouting. *J.Cereal Science*. 2008. V.47. P.6-17.
- [11] Shalachmetova G.A., Yrginbaeva Sh.M., Mamytova N.S., Galieva L.D., Kuzovlev V.A., Khakimzhanov A.A. Phytohormonal regulation of dormancy and germination of wheat seeds. *Vestnik of the KNU. Ser. Biol.* 2006. V.29. №3. P.83-87.
- [12] Appleford N.E., Lenton J.R. Hormonal regulation of  $\alpha$ -amylase gene expression in germinating wheat (*Triticum aestivum*) grains. *Physiol. Plant.* 1997. V.100. P.534-542.
- [13] Gale M.D., Lenton J.E. Pre-harvest sprouting in wheat – a complex genetic and physiological problem affecting bread-making quality of UK wheats. *Aspects of Appl.Biol. (Cereal quality)*. 1987. V.15. P.115-124.
- [14] Shi-He Xiao, Xiu-Ying Zhang, Chang-Sheng Yan, Hay Lin. Germplasm improvement for preharvest sprouting resistance in Chinese white-grained wheat: An overview of the current strategy. *Euphytica*. 2002. V.126. P.35-38.
- [15] Gilmanov M.K., Fursov O.V., Franzev A.P. Methods for studying enzymes of plants. *Alma-Ata. Science*. 1981. 91p.
- [16] Fursov O.V., Khaydarova J.S., Darkanbaev T.B. Purification, separation and some properties of  $\alpha$ -amylase components of germinating wheat grains. *Biochem. Physiol. Pflanzen*. 1986. V.81. 177-787.

TABLE I  
CHANGES IN TOTAL AMYLASE ACTIVITY IN GRAINS OF DIFFERENT WHEAT CULTIVARS AND LINES UNDER THE INFLUENCE OF HIGH HUMIDITY AND LOW TEMPERATURE

Wheat cultivar	Amylolytic activity, U/ml h				
	Control Day 0	Day 3	Day 7	Day 11	Control Day 11
Saratovskaya 29	212.80 ± 78.84	820.20 ± 34,44	775.80 ± 24,03	3638.40 ± 167,35	227.20 ± 12,03
Kazakhstanskaya 10	241.60 ± 10,63	754.20 ± 25,64	706.80 ± 27,92	2534.40 ± 101,38	235.60 ± 9,4
Kazakhstanskaya rannya	235.60 ± 8,95	583.60 ± 24,51	784.00 ± 34,49	1407.60 ± 54,95	224.80 ± 7,34
Kaiyr	220.00 ± 8,80	567.60 ± 18,67	573.00 ± 23,49	1519.20 ± 54,98	229.40 ± 8,47
Almaken	220.40 ± 9,24	637.20 ± 22,93	581.00 ± 22,07	1256.40 ± 52,12	205.20 ± 7,79
Yrym	222.40 ± 8,67	616.20 ± 24,03	525.60 ± 15,22	468.00 ± 21,06	222.10 ± 9,10
Lutescens 70	230.00 ± 9,20	622.20 ± 26,75	536.80 ± 16,08	773.80 ± 30,56	220.40 ± 7,46
Lutescens 462	228.40 ± 8,91	729.60 ± 30,64	853.80 ± 24,02	3048.00 ± 975,36	226.00 ± 10,39
Lutescens 314.	217.40 ± 9,78	679.20 ± 24,45	629.40 ± 22,37	684.00 ± 33,65	225.80 ± 6,13
Lutescens 157	209.40 ± 8,38	414.00 ± 16,97	667.20 ± 24,01	1128.00 ± 43,99	208.60 ± 7,48
no. 132 winter	230.00 ± 9,68	1600.80 ± 62,43	1515.60 ± 57,51	2246.40 ± 89,84	229.60 ± 7,78
no. 132 spring	243.00 ± 10,45	1736.40 ± 69,44	1207.20 ± 48,28	2431.20 ± 92,37	236.60 ± 8,28
no. 138 winter	229.00 ± 8,24	1286.40 ± 50,15	1090.80 ± 45,76	2580.00 ± 105,78	226.60 ± 9,04
no. 138 spring	268.20 ± 9,92	899.60 ± 34,16	966.00 ± 41,73	2071.20 ± 86,98	246.60 ± 9,84

TABLE II  
CHANGES IN TOTAL  $\alpha$ -AMYLASE ACTIVITY IN GRAINS OF DIFFERENT WHEAT CULTIVARS AND LINES UNDER THE INFLUENCE OF HIGH HUMIDITY AND LOW TEMPERATURE

Wheat cultivar	Amylolytic activity, U/ml h				
	Control Day 0	Day 3	Day 7	Day 11	Control Day 11
Saratovskaya 29	4.72± 0,18	26.18 ± 1,07	88.02 ± 2,81	1713.60 ± 71,97	4.16± 0,18
Kazakhstanskaya 10	5.66± 0,22	15.14 ± 0,59	62.28 ± 19,02	888.00 ± 38,18	5.99± 0,25
Kazakhstanskaya rannya	4.89± 0,16	3.07 ± 0,13	4.62 ± 0,07	418.08 ± 16,30	3.91±0,15
Kaiyr	3.82± 0,14	7.40 ± 0,27	6.21± 0,23	525.12 ± 21,03	3.76± 0,13
Almaken	5.57± 0,13	5.12 ± 0,20	5.61± 0,22	321.52 ± 10,44	3.71± 0,13
Yrym	4.74± 0,19	3.19 ± 0,14	5.00 ± 0,19	126.72 ± 4,43	3.18± 0,13
Lutescens 70	4.30± 0,14	2.65 ± 0,11	2.00 ± 0,12	432.00 ± 16,76	4.56± 0,20
Lutescens 462	4.85± 0,18	12.28 ± 0,51	13.76 ± 0,53	752.40 ± 3,08	4.34± 0,18
Lutescens 314	3.78± 0,17	6.42 ± 0,24	6.81± 0,27	83.76 ± 3,22	4.08± 0,16
Lutescens 157	7.49± 0,30	5.64 ± 0,25	37.26 ± 1,56	23.80 ± 0,95	3.13± 0,13
no. 132 winter	8.01± 0,32	207.00 ± 8,52	203.76 ± 8,35	711.60 ± 29,86	6.14± 0,27
no. 132 spring	8.13± 0,29	269.60 ± 10,29	249.50± 9,48	629.40 ± 27,67	6.06± 0,24
no. 138 winter	8.25± 0,31	157.32 ± 5,65	121.50 ± 5,10	125.40 ± 52,66	3.93± 0,13
no. 138 spring	8.13± 0,31	169.20 ± 6,63	209.70 ± 8,80	645.00 ± 26,44	7.82± 0,30

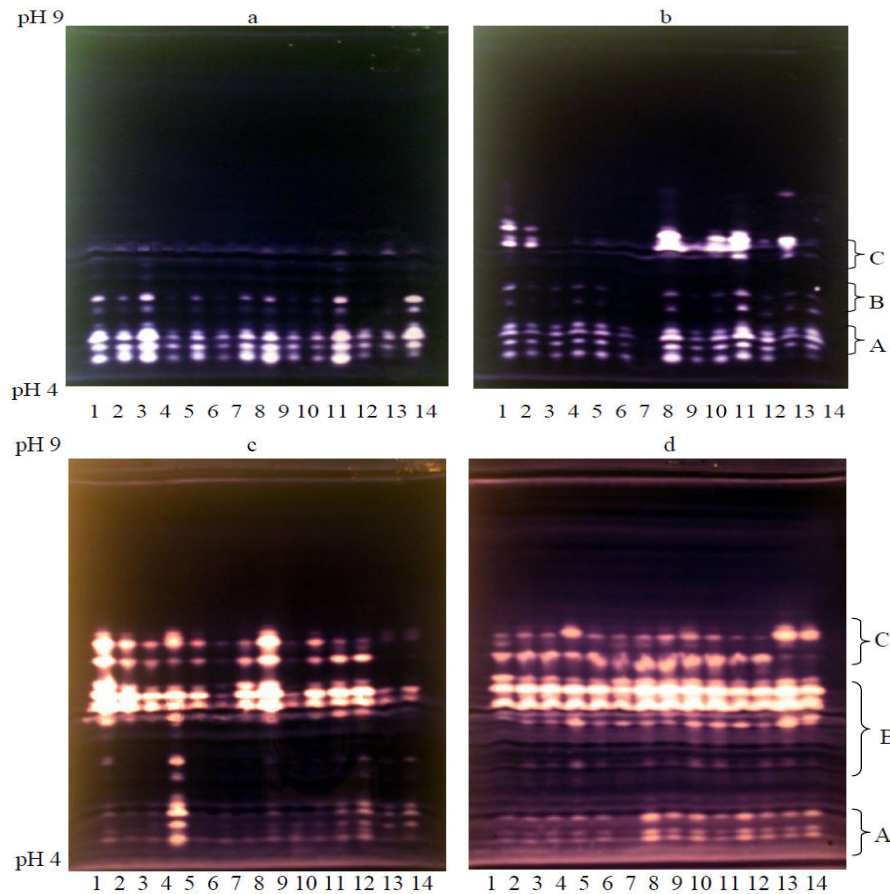


Fig. 1 Isoelectrofocusing of  $\alpha$ -amylase of different wheat cultivars and lines  
a – control (no treatment); b, c and d – day 3, 7 and 11 of seed treatment respectively by low temperature and high humidity;  
1-14 – wheat cultivars: Saratovskaya 29, Kazakhstanskaya 10, Kazakhstanskaya rannya, Kaiyr, Almaken, Yrym, Lutescens 70, Lutescens 462, Lutescens 314, no. 132 winter, no. 132 spring, no. 138 winter, no. 138 spring.  
A, B and C – isoenzymic groups of  $\alpha$ -amylase

# CFD Study of Operating Conditions in a Fixed Bed Fischer-Tropsch Synthesis Reactor

Ali Reza Miroliaei, Farhad Shahraki, Hossein Atashi, and Ramin Karimzadeh

**Abstract**—A computational fluid dynamics model has been used for study of carbon monoxide conversion in a fixed bed Fischer-Tropsch reactor. The reaction rate expressions were used based on power law. The reactions were assumed to be surface reaction type in the simulations. Effects of temperature and feed flow rate on CO conversion and yield of products were investigated. The mass fraction of species was also predicted using CFD model. It was observed that CO conversion increases with increasing temperature and decreasing mass flow rate. The values of ethylene and propylene increased with increasing temperature as well. The CFD results are in good agreement with experimental data

**Keywords**—Computational fluid dynamics, Fischer-Tropsch synthesis, Fixed bed reactor

## I. INTRODUCTION

THE Fischer-Tropsch Synthesis (FTS) is the process that the synthesis gas, a mixture of carbon-monoxide and hydrogen, obtained from natural gas, coal and biomass is converted to a mixture of hydrocarbons. Fuels produced from the FTS are of high quality due to a very low aromaticity and absence of sulfur [1]. The FTS process consists of either low temperature Fischer-Tropsch process, operated at 200-250 °C, or high temperature Fischer-Tropsch process, operated at 300-350 °C, depending on the type of the required products. Three reactor types, including multi-tubular fixed bed reactor, slurry bubble column reactor and fluidized bed reactors are used for the FTS process. The FTS process is performed on cobalt or iron based catalysts [2]-[3]. The process variables such as gas velocity, catalyst density, total pressure and hydrogen to carbon monoxide ratio affect the product distribution. Pina et al. [4] studied the effect of heat flux on the performance of an industrial methane steam reformer using a one-dimensional model. They found that the profile of heat flux along the axial direction of the reactor greatly affected the methane conversion and the tube wall temperature. Wang et al. [5] proposed a one-dimensional heterogeneous reactor model to simulate the performance of fixed bed reactors for

hydrocarbon production. Dixon et al. [6] studied diffusion and reaction for the endothermic methane steam reforming in a fixed bed reactor. They observed that the strong temperature gradient happens in the particles placed near the tube wall. Jess and Kern [3] used a two-dimensional pseudo-homogeneous model for comparison the performance of Co and Fe based catalysts in multi-tubular fixed bed reactor. They observed that the effective rate of reaction with Co is slightly higher than with Fe. Guettel and Turek [7] compared different reactor types. They used a one-dimensional model in their simulations. Shi et al. [8] used n-hexadecane as feed for the production of hydrogen. They found that the thermal conductivity of solid catalyst layer affects the temperature profile in the reactor, but its effect on product hydrogen concentration is negligible. Arzamendi et al. [9] used the combination of the steam reforming and combustion of methane in a catalytic microchannel reactor. They considered the effect of the gas velocity, catalyst load, steam to carbon ratio and flow arrangement on the microchannel performance. Duran et al. [10] developed a CFD model for predicting the performance of annular reactors with surface reaction. They studied several hydrodynamic models to predict of kinetic behavior of the reactor in laminar and turbulent flow regimes. In this work the CFD analysis of the Fischer-Tropsch synthesis is investigated in a fixed bed reactor for production of light olefins. The effects of temperature and feed flow rate on CO conversion and yield of products have been studied under laminar flow conditions. The CFD results have been compared with experimental data [11].

## II. EXPERIMENTAL SET-UP

The kinetic measurements were carried out in a fixed bed reactor. The schematic of the experimental set-up is shown in Fig 1. Three mass flow controllers equipped with a four-channel control panel were used to adjust automatically the flow rate of the inlet gases comprising CO, H<sub>2</sub> and N<sub>2</sub> with purity of 99.999%. The mixed gases passed into the reactor tube, which was placed inside a tubular furnace. The reactor tube was constructed from stainless steel tubing with the catalyst bed situated in the middle of the reactor. Reactant and product steams were analyzed on-line using a gas chromatograph.

Alireza Miroliaei is with the Department of Chemical Engineering, University of Sistan and Baluchestan, P.O. Box 98164-161, Zahedan, Iran (phone: +98 541 2447039; fax: +98 541 2447186; e-mail: armiroliaei@mail.usb.ac.ir).

Farhad Shahraki is with the Department of Chemical Engineering, University of Sistan and Baluchestan, P.O. Box 98164-161, Zahedan, Iran (phone: +98 541 2447039; fax: +98 541 2447186; e-mail: fshahraki@eng.usb.ac.ir).

Hossein Atashi is with the Department of Chemical Engineering, University of Sistan and Baluchestan, Zahedan, Iran (phone: +98 541 2443739, fax: +98 541 2443739, e-mail: h.ateshy@hamoon.usb.ac.ir).

Ramin Karimzadeh is with the Department of Chemical Engineering, University of Tarbiat Modares, P.O. Box 14155-4838, Tehran, Iran (Phone: +98 21 82883315, fax: +98 21 88006544, e-mail: ramin@modares.ac.ir).

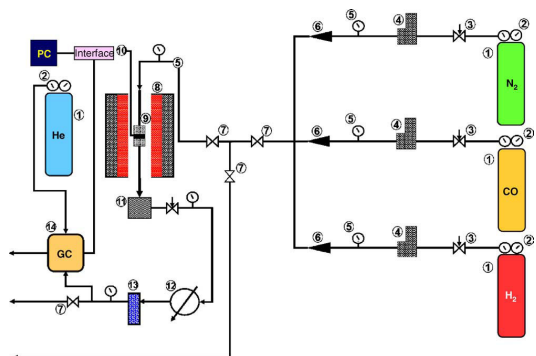


Fig. 1 Schematic representation of the reactor used: (1) gas cylinders, (2) pressure regulators, (3) needle valves, (4) mass flow controllers (MFC), (5) monometers, (6) non returns valves, (7) ball valves, (8) tubular furnace, (9) reactor, (10) catalyst bed, (11) trap, (12) condenser, (13) silica gel column and (14) gas chromatograph (GC)

### III. CFD MODELING

#### A. Governing equations

There are several commercial CFD codes such as finite element, finite difference and finite volume for process simulation. In this study, we used finite volume technique for solving the equations. The general conservation equations consist of:

- Continuity equation

$$\frac{\partial \rho}{\partial t} + \frac{\partial(\rho u_i)}{\partial x_i} = 0$$

- Momentum equation

$$\frac{\partial(\rho u_i)}{\partial t} + \frac{\partial(\rho u_i u_j)}{\partial x_j} = -\frac{\partial P}{\partial x_i} + \frac{\partial \tau_{ij}}{\partial x_j} + \rho g_i \quad (1)$$

- Energy equation

$$\frac{\partial(\rho h)}{\partial t} + \frac{\partial(\rho u_i h)}{\partial x_i} = \frac{\partial}{\partial x_i} \left( k_f \frac{\partial T}{\partial x_i} - \sum_j h_i J_{ij} \right) +$$

$$u_i \frac{\partial p}{\partial x_i} + S_h$$

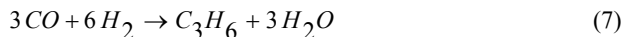
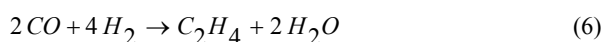
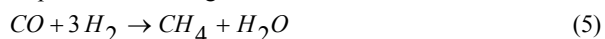
In this equation  $S_h$  includes heat of chemical reaction, any interphase exchange of heat, and any other user-defined volumetric heat sources.

- Species transport equation

$$\frac{\partial}{\partial t} (\rho Y_i) + \frac{\partial(\rho u_i Y_i)}{\partial x_i} = -\frac{\partial J_{ij}}{\partial x_i} + R_i \quad (4)$$

where  $J_i$  is the diffusion flux of species  $i$  and  $R_i$  is the net rate of production of species  $i$  by chemical reaction [12]-[13].

The FTS can be regarded as a surface polymerization reaction since monomer units are formed from the reagents in situ on the surface of the catalyst. The equations of chemical reactions are expressed according to:



The reaction rates have also been described by using power law rate equations and a function of the concentrations of carbon monoxide and hydrogen as follows:

$$R_i = k_i \exp\left(\frac{-E_i}{RT}\right) C_{CO}^m C_{H_2}^n \quad (8)$$

The values of kinetic parameters obtained by linear regression analysis are given in table I.

TABLE I  
VALUES OF KINETIC PARAMETERS

Product	$k_i$	$E_i$ (J / kgmol)	$m$	$n$
CH4	$3.30551 \times 10^{-6}$	$27.38 \times 10^6$	-0.30135	1.0951
C2H4	$2.65611 \times 10^{-4}$	$46.31 \times 10^6$	0.42481	0.52695
C3H6	$3.21193 \times 10^{-4}$	$45.34 \times 10^6$	0.51780	0.54717

#### B. Geometry and boundary conditions

The 3-D geometry comprising 44 spherical particles with 0.0038 m diameter was used in CFD simulations. The geometry and unstructured tetrahedral mesh were generated by using commercial software, GAMBIT 2.0.4. The continuity, momentum, energy and species equations were solved by using commercial CFD package, ANSYS FLUENT 12.0.16. Physical properties of gaseous species were defined as temperature-dependant. For mixture material, mass weighted-mixing law for thermal conductivity and viscosity, mixing-law for specific heat capacity were selected. The boundary conditions were used at steady-state flow and equal to the boundary conditions for physical experiments. The condition of mass flow rate was used at the reactor inlet. Species mole fraction ratios of carbon monoxide, hydrogen and nitrogen were 0.2, 0.4 and 0.4 respectively. At the reactor outlet, outlet flow boundary condition was used. No-slip boundary condition was applied at the walls. The pressure-velocity coupling was performed by the SIMPLE scheme. Second-order upwind schemes were used for the advection terms in the momentum, energy and species equations.

### IV. RESULTS AND DISCUSSION

In this section, the effects of temperature and mass flow rate on CO conversion and yield of products are shown in a temperature range of 463.15-523.15 K and the mass flow rate of  $1.9-6.5 \times 10^{-6}$  kg/s.

The effects of temperature on carbon monoxide conversion have been shown in Fig. 2. It can be seen from Fig. 2 that with increasing temperature, the conversion of carbon monoxide increases. According to kinetic theory of gases, the kinetic energy of molecules increases with increasing temperature, consequently the value of CO consumption increases.

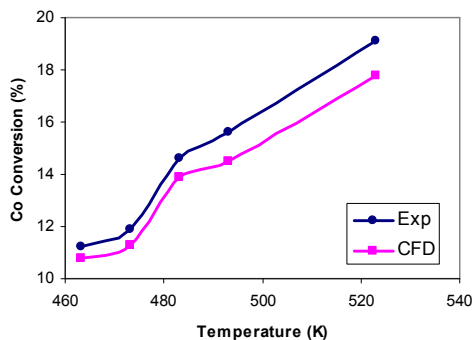


Fig. 2 Carbon monoxide conversion as a function of temperature

Fig. 3 shows the effects of feed flow rate on carbon monoxide conversion at three different mass flow rates. As shown in Fig. 3, with increasing mass flow rate, CO conversion decreases because the residence time of reactants decreases and the flow channeling and vortex also increase into the bed.

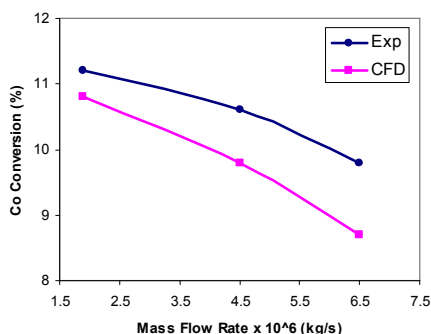
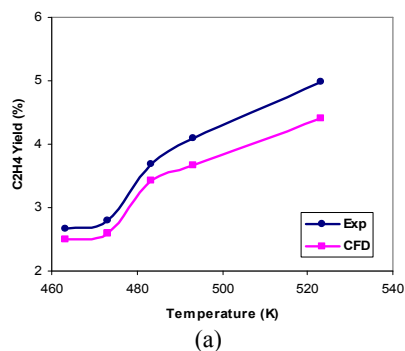


Fig. 3 Carbon monoxide conversion as a function of mass flow rate

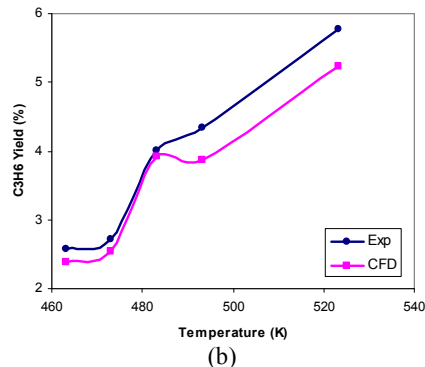
The yield of the products has been shown in Fig. 4. The yield (%) towards the components on CO conversion-basis was calculated according to:

$$\text{Yield of } i \text{ product (\%)} = (\text{CO conversion}) \times (\text{Selectivity of } i \text{ product}) \times 100 \quad (9)$$

It can be seen that the values of ethylene and propylene increase with increasing temperature.



(a)



(b)

Fig. 4 Yield of products as a function of temperature

The mass fraction of species has been indicated in Fig. 5. As can be seen the mass fraction of species increases with temperature because the reactions progress. As the temperature increases, the mass fraction of methane increases slowly, while the mass fraction of ethylene and propylene increases rapidly.

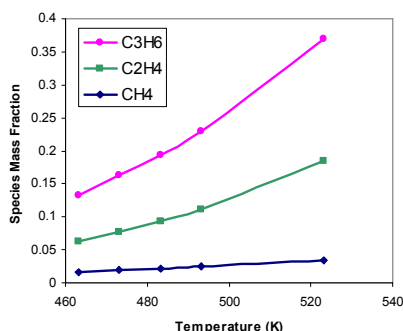


Fig. 5 Mass fraction of products as a function of temperature

## V. CONCLUSIONS

The comparison between the CFD results and the experimental data was carried out for the Fischer-Tropsch synthesis process. The fixed bed reactor was used for production of light olefins such as ethylene and propylene. The effects of temperature and feed flow rate on the yield of products were investigated. It was observed that the value of CO consumption increased with increasing temperature but the value of that decreased with increasing mass flow rate because the fluid residence time decreases into the bed. The mass fraction of species increased with increasing temperature as well. The CFD values are in good agreement with the experimental data [11].

## REFERENCES

- [1] M. Ahmadi Marvast, M. Sohrabi, S. Zarrinpashne, Gh. Baghmisheh, "Fischer-Tropsch synthesis: modeling and performance study for Fe-HZSM5 bifunctional catalyst," Chem. Eng. Technol. Vol. 28, pp. 78-86, 2005.
- [2] S. H. Kang, J. W. Bae, K. J. Woo, P.S. Sai Prasad, K. W. Jun, "ZSM-5 supported iron catalysts for Fischer-Tropsch production of light olefin," Fuel Proc. Tech. vol. 91, pp. 399-403, 2010.

- [3] A. Jess, C. Kern, "Modeling of multi-tubular reactors for Fischer-Tropsch synthesis," *Chem. Eng. Technol.* Vol. 32, pp. 1164-1175, 2009.
- [4] J. Pina, N.S Schbib, V. Bucala, D.O. Borio, "Influence of the heat flux profiles on the operation of primary steam reformers," *Ind. Eng. Chem. Res.* Vol. 40, pp. 5215-5221, 2001.
- [5] Y.N. Wang, Y.Y. Xu, Y.W. Li, Y.L. Zhao, B.J. Zhang, "Heterogeneous modeling for fixed-bed Fischer-Tropsch synthesis: Reactor model and its applications," *Chem. Eng. Sci.* vol. 58, pp. 867-875, 2003.
- [6] A.G. Dixon, M.E. Taskin, E.H. Stitt, M. Nijemeisland, "3D CFD simulations of steam reforming with resolved intraparticle reaction and gradients," *Chem. Eng. Sci.* vol. 62, pp. 4963-4966, 2007.
- [7] R. Guettel, T. Turek, "Comparison of different reactor types for low temperature Fischer-Tropsch synthesis: A simulation study," *Chem. Eng. Sci.* vol. 64, pp. 955-964, 2009.
- [8] L. Shi, D.J. Bayless, M.E. Prudich., "A CFD model of autothermal reforming," *Int. J. Hydrogen Energy*, vol. 34, pp. 7666-7675, 2009.
- [9] G. Arzamendi, P.M. Dieguez, M. Montes, J.A. Odriozola, E.F.S. Aguiar, L.M. Gandia, "Methane steam reforming in a microchannel reactor for GTL intensification: A computational fluid dynamics simulation study," *Chem. Eng. J.* vol. 154, pp. 168-173, 2009.
- [10] J. Esteban Duran, M. Mohseni, F. Taghipour, "Modeling of annular reactors with surface reaction using computational fluid dynamics (CFD)," *Chem. Eng. Sci.* vol. 65, pp. 1201-1211, 2010.
- [11] H. Atashi, F. Siami, A.A. Mirzaei, M. Sarkari, "Kinetic study of Fischer-Tropsch process on titania-supported cobalt-manganese catalyst," *J. Ind. Eng. Chem.* vol. 16, pp. 952-961, 2010.
- [12] A.G. Dixon, M. Nijemeisland, E.H. Stitt, "Packed tubular reactor modeling and catalyst design using computational fluid dynamics," *Advances in Chemical Engineering*, vol. 31, pp. 307-389, 2006.
- [13] ANSYS, Inc. ANSYS FLUENT 12.0 theory guide, species transport and finite-rate chemistry, ANSYS, Inc. 2009.